NACA

RESEARCH MEMORANDUM

DOWNWASH AND SIDEWASH FIELDS BEHIND CRUCIFORM WINGS

By John R. Spreiter

Ames Aeronautical Laboratory
Moffett Field, Calif.

NATIONAL ADVISORY COMMITTEE FOR AERONAUTICS

WASHINGTON
January 7, 1952

NATIONAL ADVISORY COMMITTEE FOR AERONAUTICS

RESEARCH MEMORANDUM

DOWNWASH AND SIDEWASH FIELDS BEHIND CRUCIFORM WINGS

By John R. Spreiter

SUMMARY

A brief account is presented of the results of theoretical and experimental investigations of the flow fields behind lifting plane and cruciform wings. Particular attention is focussed on wings of low aspect ratio. It is shown that the deformation of the vortex sheet behind a plane wing consists essentially of a rolling up at the edges. For banked cruciform wings, however, it is shown that, in addition to this effect, the vortices from the upper wing tips pass downward between those from the lower tips. Certain anomalous behaviors of the pitching-moment characteristics of a typical missile configuration are shown to be explainable on the basis of these results.

INTRODUCTION

A rational approach to stability and control problems requires an accurate knowledge of the induced flow field behind a lifting wing. In the absence of separation, reliable engineering solutions to this problem have been known for conventional airplane configurations for a long time. For missile configurations, however, the old methods often fail to yield accurate results. The difficulties arise largely from the presence of complicated vortex wake patterns resulting from the use of low-aspect-ratio wings and cruciform wings. The present paper will describe some results of recent work on these problems. To date most of the theoretical analysis has been for the wing alone but similar work is now progressing for plane and cruciform wing and body combinations. The results obtained so far are encouraging in that they seem to indicate that most of the major effects are understandable on the basis of existing methods.

[redacted]

RESULTS AND DISCUSSION

It is generally known that vortex sheets are formed behind lifting wings and that knowledge of their strength and location is essential for the calculation of downwash and sidewash velocities. As may be observed experimentally or calculated theoretically, the vortex sheet trailing behind each panel of a wing rolls up at the edges in a manner much as illustrated in figure 1. For the plane wing or the cruciform wing banked 0° ($\varphi = 0^\circ$), the vortices eventually become essentially rolled up into two vortex-core regions as shown in the sketch on the left. For the banked cruciform wing, the vortex sheets might be presumed to roll up similarly into four vortex cores. The sketch on the right shows such a case for an angle of bank of 45° ($\varphi = 45^\circ$).

Plane Wings

Insight into the rate of deformation of the trailing vortex sheet can be gained by considering the similarity rule presented originally in reference 1. A brief resume of the results so obtained is shown in figure 2. It is found for either subsonic or supersonic speeds that the distance d from the wing trailing edge to the station where the trailing vortex sheet is deformed to any specified degree is given by the first equation where c is the root chord, A the aspect ratio, C_L the lift coefficient, b the span, and K is an unspecified constant depending on the load distribution and on the degree of wake deformation specified.

Although this equation is very simple, the implications are of considerable practical importance. As an illustrative example, compare the rate of rolling up of the vortex sheets trailing behind a rectangular wing of aspect ratio 6 with that for a triangular wing of aspect ratio 2. It will be assumed that the wings are twisted in such a manner that they have similar span loadings; then the value of K will be the same for both wings. Thus, in terms of chords, it can be seen that the trailing vortex sheet rolls up 18 times more rapidly behind the low-aspect-ratio triangular wing than behind the high-aspect-ratio rectangular wing. This is illustrated graphically in the two sketches. In both sketches, the vortices are rolled up to the same degree at the indicated sections. For the missile designer, the lesson to be learned from the preceding considerations is that the rolling up of the trailing vortex sheet must be taken into account if accurate predictions of the induced flow field behind low-aspect-ratio wings is to be accomplished. In many instances, however, the rolling up is so rapid that adequate predictions can be made by assuming that the vortices are completely rolled up at the tail location.

A detailed analysis of the behavior of vortex systems can always be made by replacing the continuous sheet of vortices with a finite number of discrete line vortices and calculating step by step the motions of each vortex. The results of such a calculation for a plane wing having elliptic span loading (or for an unbanked cruciform wing) using 20 discrete vortices are shown in figure 3. (See references 1 and 2.) It may be seen that the center of the vortex sheet becomes inclined a substantial angle below the free-stream direction. The vortex cores, however, extend downstream in nearly the free-stream direction and soon contain a major portion of the vorticity.

The behavior of the vortex sheets has been studied further by means of simple visual-flow experiments in a water tank. These experiments were conducted by driving a model wing vertically into the water at a constant velocity and photographing the water surface with a movie camera. The trace of the trailing vortex sheet was made visible by applying fine aluminum powder to the trailing edge of the wing before each run. Figure 4 shows an abridged series of photographs for a triangular wing of aspect ratio 2 at an angle of attack of 20°, corresponding to an estimated lift coefficient of approximately 0.77. The distance behind the wing, in chords, is indicated by the values of d/c given below each figure. The projections in the free-stream direction of the wing-tip positions are indicated in the photographs by the intersections of the vertical lines and the horizontal markers. These photographs clearly illustrate the rapidity with which the trailing vortex sheet rolls up behind a low-aspect-ratio wing and further emphasizes the fact that the vortex cores extend rearward in very nearly the free-stream direction. These conclusions have been confirmed by a number of wind-tunnel tests conducted by Wetzel and Pfyl (reference 3) in the Ames 6- by 6-foot supersonic tunnel and by Spahr in the Ames 1- by 3-foot supersonic tunnel.

An example of the effect on missile stability resulting from the nonlinear behavior of the downwash field is illustrated in figure 5. This figure shows the variation of the pitching-moment coefficient C_m with angle of attack α for the Sparrow missile as determined from measurements at a Mach number of 1.4 made in the Ames 6- by 6-foot supersonic tunnel by Edwards. (See reference 4.) Also shown in figure 5 are corresponding theoretical results calculated by Edwards. The forces and moments on the wing and body were determined by using slender wing-body theory (reference 5) in a manner similar to that of Nielsen, Katzen, and Tang (reference 6). The trailing vortex sheet was assumed to be completely rolled up into two line vortices lying at the 0.8-semispan station and extending rearward in the free-stream direction as shown in the small auxiliary figures. The forces on the tail were computed with the use of strip theory in accordance with some theorems of Lagerstrom and Van Dyke (reference 7). It is seen that these methods lead to adequate predictions of the pitching-moment variations with angle of attack.

Cruciform Wings

The analysis of the induced flow field behind banked cruciform wings may be carried out by methods completely analogous to those used for a plane wing (or unbanked cruciform wing). As for the plane wings, the first step is always to determine the span loading. This can readily be done since the loading on each panel of a cruciform wing is the same, to the order of accuracy of linear theory, as on the panels of a plane wing inclined at equal angles of attack and bank. (See reference 5.) These considerations determine the vorticity distribution directly behind the trailing edge. Before the induced flow field farther behind the wing can be calculated, it is necessary to ascertain the subsequent behavior of the trailing vortex sheet.

Figure 6 presents some of the results of a detailed calculation of the behavior of the trailing-vortex system behind a cruciform arrangement of triangular wings banked 45°. These results were obtained by approximating the vortex wake by a total of 40 discrete vortices and calculating their subsequent behavior by a step-by-step process. It can be seen that the vortex sheets roll up into four regions of more or less concentrated vorticity, the vortex cores. Just as for the plane-wing results, the vortex cores extend rearward from the trailing edge in nearly the free-stream direction while the center of the vortex sheet becomes inclined a substantial angle below the free-stream direction. Because the course of the vortex sheets near the plane of symmetry becomes too complex to follow the 40-vortex approximation, the vortex wake is dashed through this region. Note in particular that the vortices in this region do not appear to be rolling up into the four concentrated tip vortices.

Figure 7 presents a series of photographs showing the results of water-tank experiments to determine the behavior of the trailing vortex sheets behind a cruciform wing banked 45°. The wings were triangular in plan form, had an aspect ratio of 2, and were inclined at an angle of attack of 16.9°. At the lesser distances behind the wing, the customary rolling-up tendencies are to be observed. Again it appears that the vortices near the plane of symmetry fail to roll up into the tip vortices. At greater distances behind the wing, a new effect which will be called "leapfrogging" is to be observed. The vortex cores from the upper wing tips pass downward between those from the lower wing tips. In this case, the "leapfrog" distance (defined as the distance from the wing trailing edge to the station where the vortex cores from the upper panels pass between those from the lower panels) is only 4.8 chords. It is interesting to recall that this phenomenon is closely related to the similar behavior of vortex rings described by Helmholtz in 1858 in his classical paper on vortex motion.

In order to gain a greater understanding of the leapfrogging phenomenon, an analysis has been carried out by Sacks in which the behavior of four- and six-vortex approximations to the trailing vortex system are determined in full detail (see reference 8). One of his most significant results is the variation of leapfrog distance with C_L/A^2 for triangular cruciform wings having subsonic leading edges (see fig. 8). In this figure, the long- and short-dash-line curve indicates the results of the four-vortex calculations and the points represent values obtained from the water-tank experiments. It is seen that the four-vortex approximation yields good agreement for small C_L/A^2 but that significant differences appear at larger C_L/A^2. Sacks has examined the origin of this discrepancy and concluded that a major contribution is due to the failure of the portion of the vortex sheet near the plane of symmetry to roll up into the four vortex cores as assumed. As C_L/A^2 increases, an increasing amount of vorticity near the wing root tends to roll up into an additional pair of vortex cores as can be seen in the water-tank photographs of figure 7. The leapfrog distance was therefore calculated anew assuming a six-vortex approximation to the rolled-up vortex sheet. The results of these calculations are also shown in figure 8. It is seen that the new results are in closer agreement with the experimental data obtained with the water tank. For comparison, the distance required for the vortex sheet behind a plane wing to become essentially rolled up is also shown. (See references 1 and 9.) The principal lesson to be learned from this figure is that the leapfrog distance decreases rapidly with increasing C_L/A^2. The numerical values are such that the leapfrogging phenomenon is only of practical importance in missile designs having wings of particularly low aspect ratio and could be avoided, if desired, in most cases by a slight increase in aspect ratio.

The resultant effect on the longitudinal stability of the Sparrow missile with wings banked 45° is shown in figure 9. This figure, taken from reference 4 by Edwards, shows the variation of C_m with α as determined from measurements at a Mach number of 1.4 in the Ames 6- by 6-foot supersonic tunnel and from theoretical calculations similar to those described earlier in connection with figure 5. In performing these calculations, Edwards again assumed that the trailing vortices were completely rolled up into four trailing vortices extending rearward in the direction of the free stream. A slight correction to the lateral position of the lower pair of vortices was then applied to account for the early stages of leapfrogging action. It may be seen from this graph that the results so obtained were highly satisfactory in duplicating a distinctly nonlinear pitching-moment curve. The peak of the pitching-moment curve occurred when the vortex cores from the lower panels of the wing were in the plane of the horizontal tail as shown in the sketch of the missile. The assumption that the vortex

distribution at the tail could be adequately represented by four vortices and that leapfrogging effects were of only secondary importance is in accord with the graph of Sacks shown previously in figure 8 and repeated in miniature here. The total range of Edwards' results, as indicated by the test points on the miniature graph, are seen to be principally in the region where the vortices are essentially rolled up but never approach the line indicating leapfrogging.

Figure 10 shows two schlieren photographs obtained by Spahr in the Ames 1- by 3-foot supersonic tunnel of side views of the flow about the Falcon missile. In both photographs the forward wings are at 45° angle of bank and the entire missile is at 13° angle of attack. The cores of the vortices trailing behind both the upper and lower wing panels can be clearly distinguished in both photographs. For the missile with moderate-aspect-ratio wings, the photograph on the left shows that the vortices fall short of leapfrogging at the tail location. For the model with very low-aspect-ratio wings, however, the photograph on the right shows that the vortices pass between each other at the tail station. For purposes of comparison, the leapfrog station has been calculated for both cases by using Sack's results for the wing alone together with theoretical values for the lift of the actual wing-body combination calculated by the methods of references 5 and 6. It may be seen that these preliminary considerations, ignoring the influence of the body on the motion of the vortices, provide predicted leapfrog distances in at least sensible agreement with the experimental results.

Despite the agreement on the leapfrog distance indicated in figure 10, caution should be exercised in applying the results discussed to configurations having large bodies and small wings. Preliminary experiments with models possessing such geometric characteristics indicate some significant departures from the results just reviewed. In particular, the trailing vortex sheet sometimes breaks up into a number of more or less distinct regions of vorticity and often a prominent vortex forms behind the inner portion of the wing. Since many missiles possess the afore-mentioned geometrical configurations, both theoretical and experimental investigations are now in progress at Ames Aeronautical Laboratory to explore this subject in greater detail.

Ames Aeronautical Laboratory
National Advisory Committee for Aeronautics
Moffett Field, Calif.

[redacted]

REFERENCES

1. Spreiter, John R., and Sacks, Alvin H.: The Rolling Up of the Trailing Vortex Sheet and Its Effect on the Downwash behind Wings. Jour. Aero. Sci., vol. 18, no. 1, Jan. 1951, pp. 21-32, 72.

2. Westwater, F. L.: Rolling Up of the Surface of Discontinuity behind an Aerofoil of Finite Span. R. & M. 1692, British A.R.C., 1935.

3. Wetzel, Benton E., and Pfyl, Frank A.: Measurements of Downwash and Sidewash Behind Cruciform Triangular Wings at Mach Number 1.4. NACA RM A51B20, 1951.

4. Edwards, S. Sherman: Experimental and Theoretical Study of Factors Influencing the Longitudinal Stability of an Air-to-Air Missile at a Mach Number of 1.4. NACA RM A51J19, 1951.

5. Spreiter, John R.: The Aerodynamic Forces on Slender Plane- and Cruciform-Wing and Body Combinations. NACA Rep. 962, 1950. (See also NACA TN 1897.)

6. Nielsen, Jack N., Katzen, Elliot D., and Tang, Kenneth K.: Lift and Pitching-Moment Interference Between a Pointed Cylindrical Body and Triangular Wings of Various Aspect Ratios at Mach Numbers of 1.50 and 2.02. NACA RM A50F06, 1950.

7. Lagerstrom, P. A., and Van Dyke, M. D.: General Considerations about Planar and Non-Planar Lifting Systems. Rep. No. SM-13432, Douglas Aircraft Co., Inc., June 1949.

8. Sacks, Alvin H.: Behavior of Vortex System Behind Cruciform Wings - Motion of Fully Rolled-Up Vortices. NACA TN 2605, 1951.

9. Kaden, H.: Aufwicklung einer unstabilen Unstetigkeitsfläche. Ing. Archiv, Bd. II, Heft 2, May 1931, pp. 140-168.

Figure 1.- Views of cruciform wings and wakes.

$$\frac{d}{c} = K \frac{A}{C_L} \quad \frac{b}{c}$$

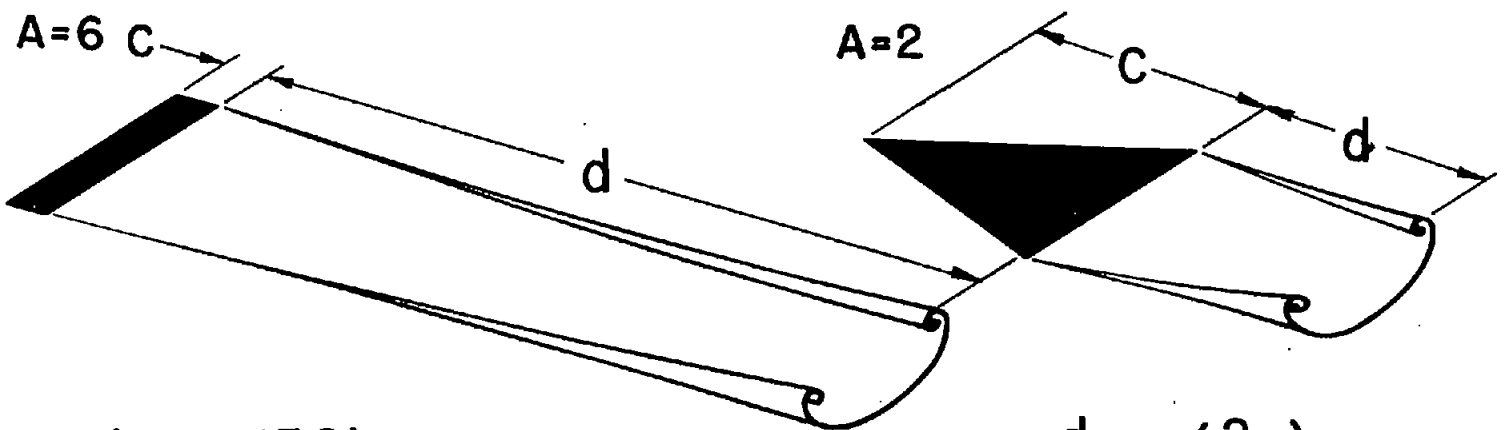

$$\frac{d}{c} = K\left(\frac{36}{C_L}\right)$$

$$\frac{d}{c} = K\left(\frac{2}{C_L}\right)$$

Figure 2.- Rate of rolling up of trailing vortex sheet, $\varphi = 0^{\circ}$.

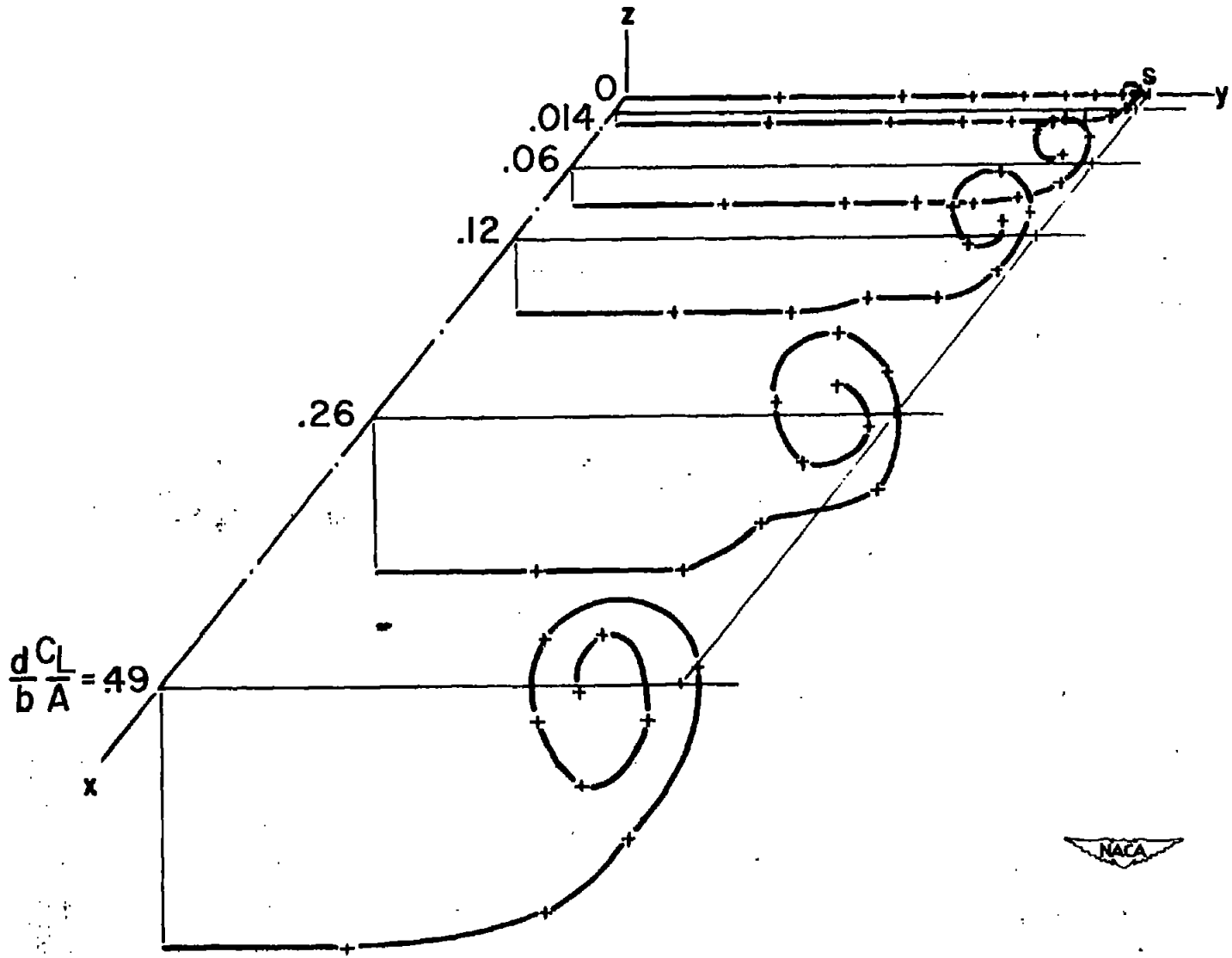

Figure 3.- Calculated shape of vortex wake for elliptic loading, $\varphi = 0^\circ$.

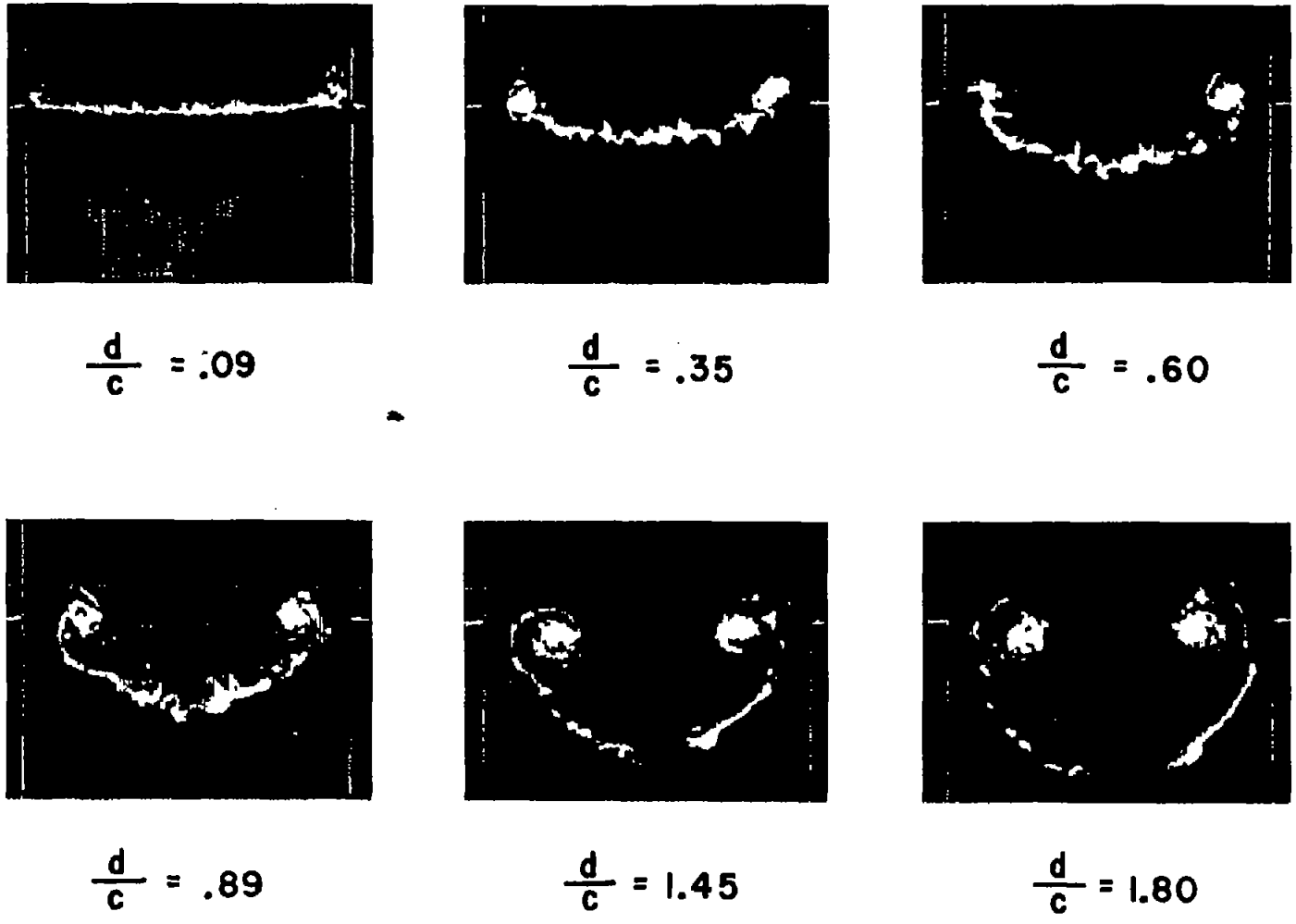

Figure 4.- Photographs of wake at various stations behind wing, $\varphi = 0^\circ$.

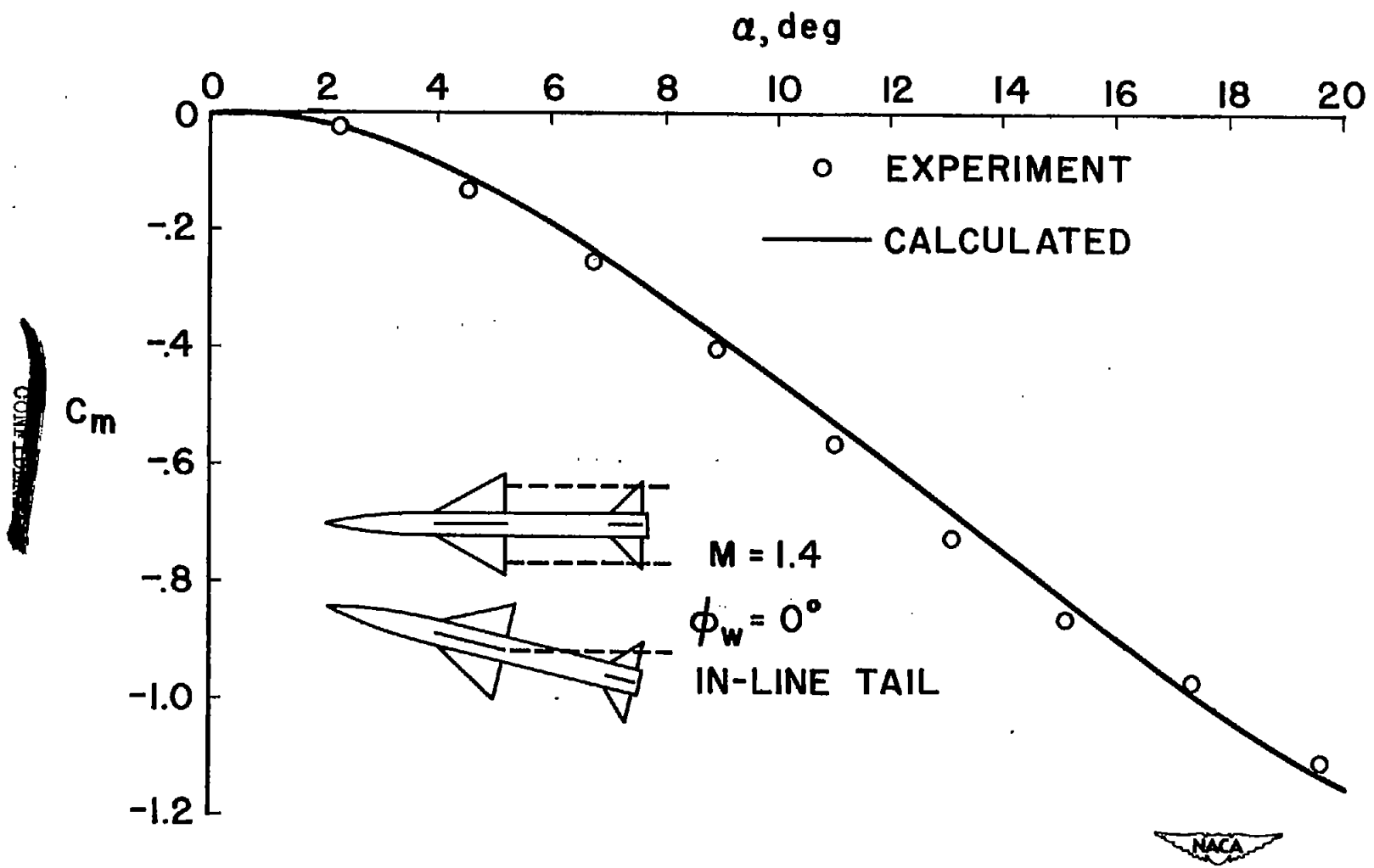

Figure 5.- Pitching-moment characteristics of a complete missile, $\varphi = 0°$.

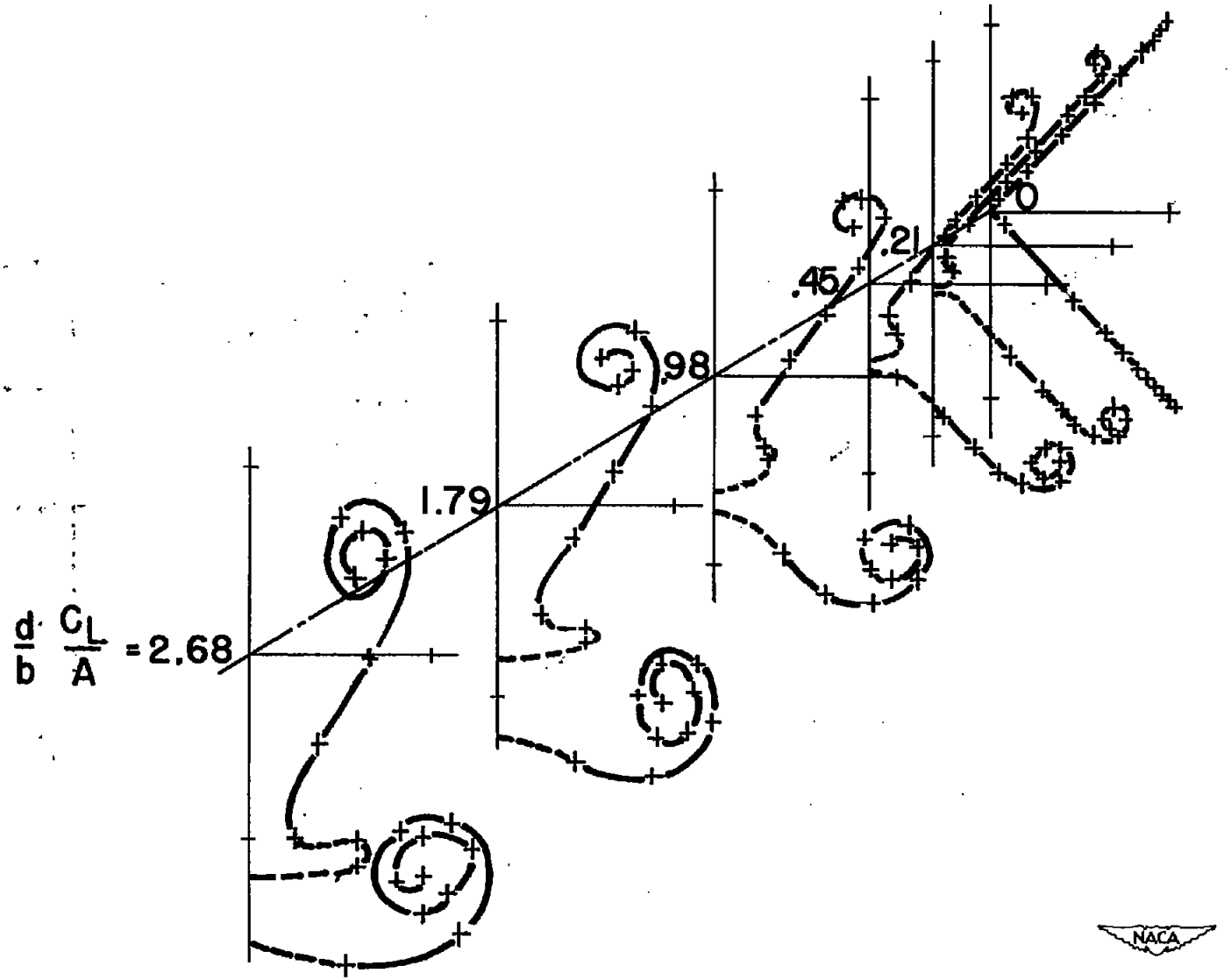

Figure 6.- Calculated shape of vortex wake of triangular cruciform wings, $\varphi = 45^\circ$.

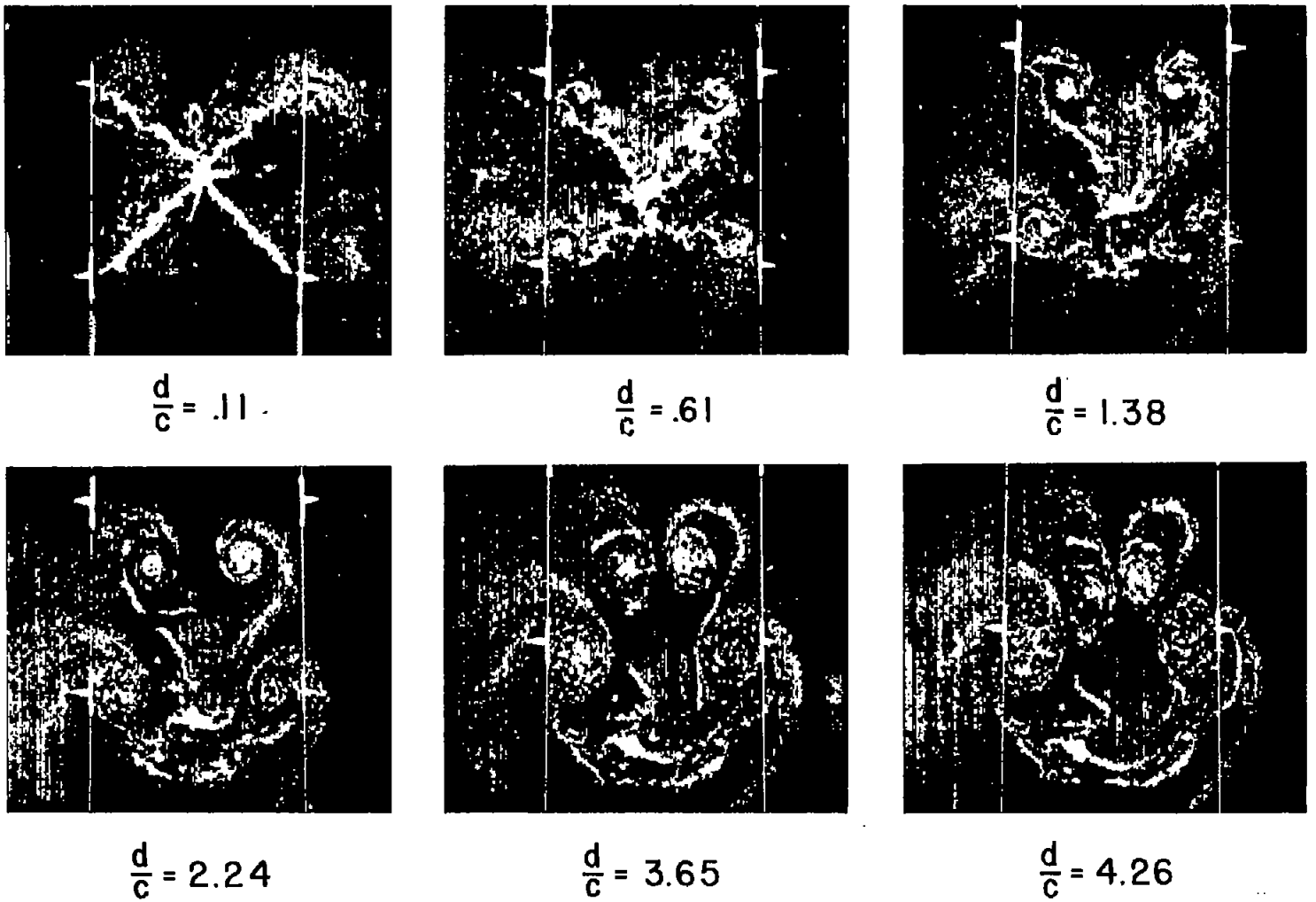

Figure 7.- Photographs of wake at various stations behind wing, $\varphi = 45°$.

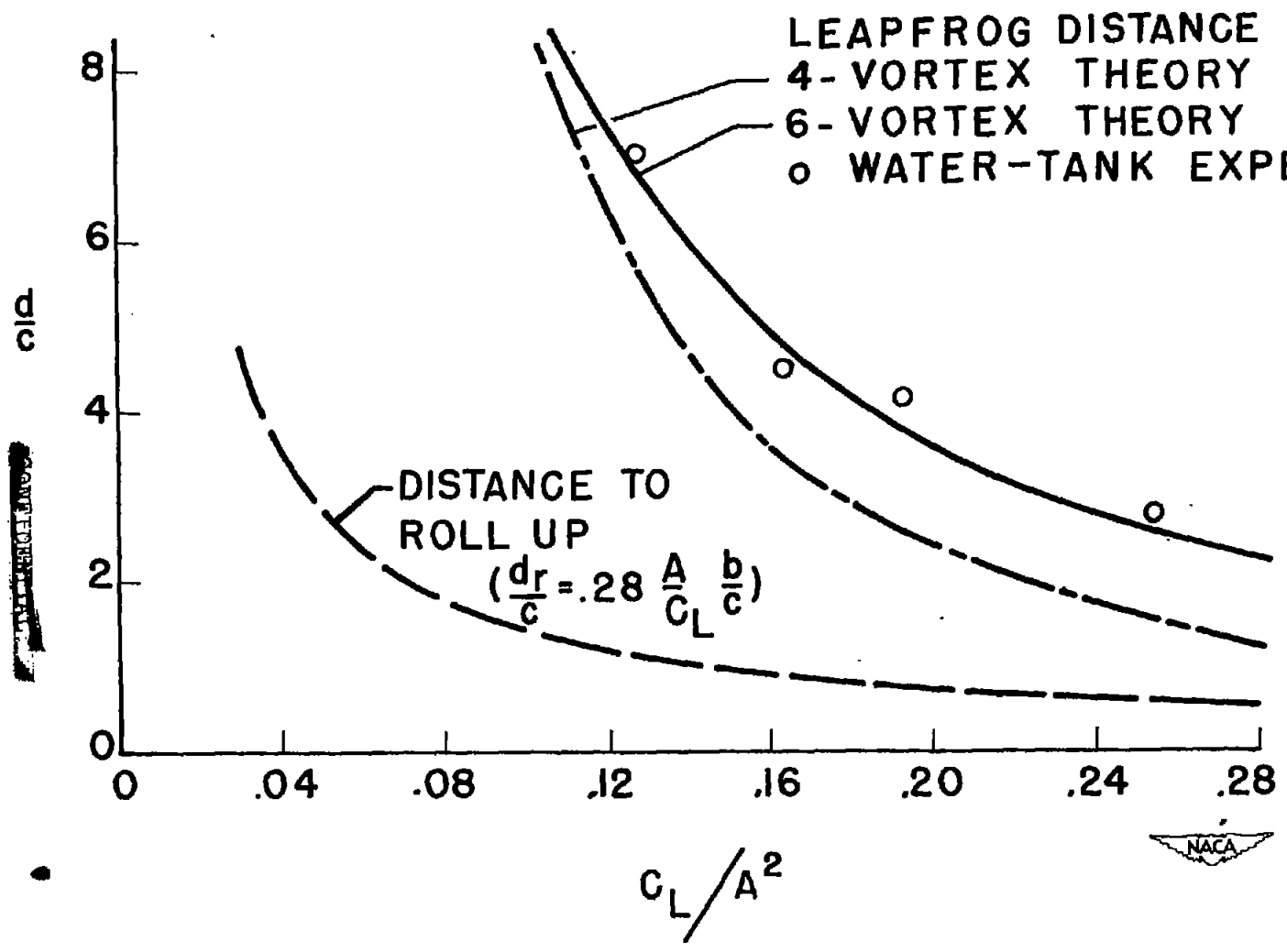

Figure 8.- Variation of leapfrog distance with C_L/A^2 for triangular cruciform wings, $\varphi = 45°$.

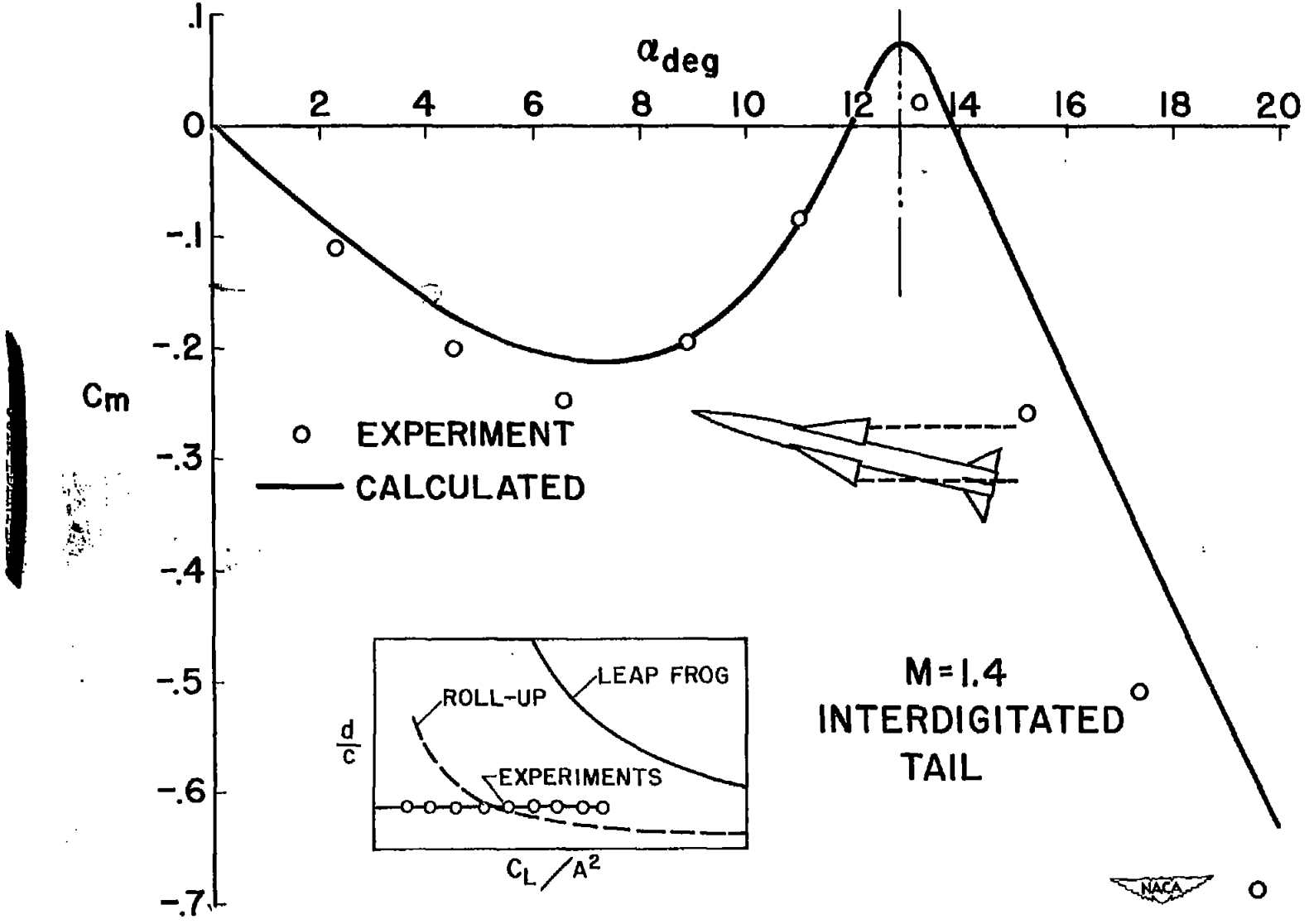

Figure 9.- Pitching-moment characteristics of a complete missile, $\varphi = 45^\circ$.

Figure 10.- Schlieren photographs illustrating leapfrog phenomenon.

NACA-Langley - 1-7-52 - 325